THE JOURNAL OF PHYSICAL CHEMISTRY B

ARTICLE

pubs.acs.org/JPCB

# Multidonor Deep-UV FRET Study of Protein−Ligand Binding and Its Potential to Obtain Structure Information

Qiang Li and Stefan Seeger*

Institute of Physical Chemistry, University of Zurich, Winterthurerstrasse 190, CH-8057 Zurich, Switzerland

**ABSTRACT:** Fluorescence resonance energy transfer (FRET) using biotinylated $\beta$-galactosidase ($\beta$GAL) as a donor and Alexa Fluor 350 (AF350) labeled avidin as an acceptor has been investigated by means of steady-state fluorescence and time-resolved fluorescence spectroscopy. The donors are readily paired with acceptors through the well-established binding affinity of biotin and avidin. The fluorescence energy transfer efficiency was determined by the donor fluorescence emission and lifetime changes in the presence and absence of acceptor. The theoretical energy transfer efficiency and theoretical average distance between donor and acceptor after noncovalent binding was calculated by taking the distribution of tryptophan residues in $\beta$GAL and avidin as well as the location of AF350 in avidin into account, which agree with the experimental data. It is shown how information of the location of the acceptor can be obtained. Further, the fluorescence intensity image of AF350 on a biotinylated $\beta$GAL-coated quartz surface through UV FRET has been recorded using deep UV laser-based fluorescence lifetime microscopy. The results demonstrate that (a) deep UV laser-based fluorescence lifetime microscopy is a simple and useful method to study UV FRET of proteins using intrinsic fluorescence, (b) structural information even in complex multidonor systems can be obtained, and (c) FRET signals can be obtained to detect binding events using the native fluorescence of proteins as multidonor systems.

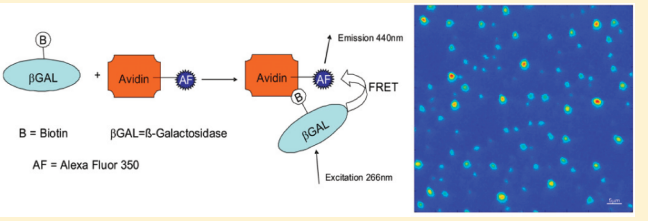


## 1. INTRODUCTION

Fluorescence resonance energy transfer (FRET) is a nonradiative process whereby an excited-state donor molecule transfers energy to a proximal ground-state acceptor through long-range dipole−dipole interaction.[1,2] FRET has become widely used in many applications of fluorescence, including medical diagnostics, DNA analysis, and optical imaging.[1] FRET is often cited as "spectroscopic ruler" due to its capability to supply accurate spatial measurements and to detect molecular complexes over distances from 10 to 100 Å, which are typically the size of a protein or the thickness of a membrane. This makes FRET useful for studying various biological macromolecules.[3−6]

The existing methods to study the interaction by FRET between two proteins are labeling techniques. Two fluorophors, one donor and one acceptor, have to be chosen and attached to a binding partner. Upon binding, the probe molecule, not primarily the molecule of interest (e.g., proteins), is detected. Although these labels are specifically designed to receive a sensitive assay, the chemical procedures involved in attachment of a label are time-consuming, expensive, and labor intensive and may lead to additional losses of valuable sample material due to purification steps. Further, chemical labeling of proteins might change their surface characteristics so that their natural activity is impaired. In other words, the labeling procedures may affect the biological activity of the molecules under investigation, especially for small proteins or peptides containing only a few epitopes. Label-free techniques have been developed in order to overcome these problems. In contrast to methods containing labels, target proteins are not labeled or altered and are detected in their native form. This label-free technique is relatively easy and cheap to perform and allows for quantitative and kinetic measurement of molecular interaction. Label-free methods are becoming an important tool for biological analysis due to their inherent merits.[7]

Most proteins contain the aromatic residues tryptophan (Trp), tyrosine (Tyr), and phenylalanine (Phe), which fluoresce in the near-UV upon excitation around 280 nm.[1] However, the intrinsic fluorescence of Tyr is about 100 times weaker than that of Trp due to a low extinction coefficient; fluorescence emission of Phe is quite weak because of the low extinction coefficient and low quantum efficiency. For proteins that contain these residues, it is often found that the emission is dominated by the contribution of the Trp residues, which emit in the range of 335−345 nm. The Trp fluorescence emission has been applied to study protein folding, enzymatic catalysis, ligand binding, and protein association.[1] Recently we showed the detection of small single molecules and single proteins without any labeling using deep UV laser-based fluorescence lifetime microscopy.[7−9] This method is also quite useful for sensitive identification of protein interactions[10,11] and for direct analysis of protein separation by gel and capillary electrophoresis.[12−14] Zauner et al.[15] exploited the sensitivity of the endogenous Trp fluorescence of type-3 copper protein toward the presence of oxygen by translating the intrinsic UV emission of the protein to label fluorophors in the

**Received:** April 15, 2011
**Revised:** October 13, 2011
**Published:** October 13, 2011

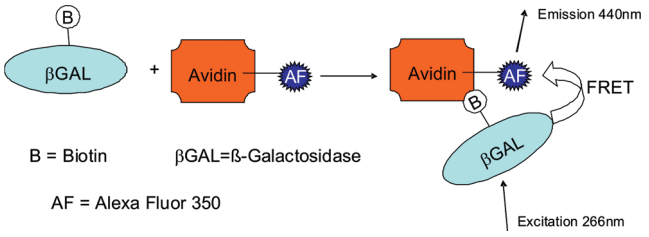


**Figure 1.** Schematic illustration of the FRET process from the biotinylated $\beta$GAL to avidin-AF350 based on the high affinity of biotin and avidin reaction.

visible range through a FRET mechanism. Two type-3 copper proteins, hemocyanins and tyrosinases, were labeled with several fluorophors (e.g., Alexa Fluor 350 (AF350), Atto 390, etc.) at the N-terminus. The Trp emission of the proteins and the fluorescence of the fluorophore labels from FRET depend on the concentration of oxygen in solution, which can be used for oxygen sensing based on FRET.

In the present report we introduce FRET using aromatic amino acids of proteins as donors after deep UV excitation. The design of biotinylated $\beta$-galactosidase ($\beta$GAL)/avidin-AF350 conjugate is shown schematically in Figure 1. There are four binding sites in each avidin molecule that can bind up to four molecules of biotin noncooperatively with very high affinity ($K_d = 1.3 \times 10^{-15}$ M).[16−18] The bond formation between biotin and avidin is widely unaffected by pH, temperature, organic solvents, and other denaturing agents. The four binding sites, together with the high affinity of the biotin−avidin interaction, help to enhance the signal strength and amplify the sensitivities of biotin−avidin-based analysis.[19,20] The biotin−avidin technique is a useful tool in specific targeting applications and assay design.[21−24]

$\beta$GAL was chosen as the donor mainly because of its strong fluorescence emission from abundant Trp residues at UV excitation. It is an enzyme containing 156 Trp residues and is widely distributed in microorganisms, animals, and plants.[25] This enzyme is a tetramer of four identical subunits with a monomer molecular mass of 116 352. Within each subunit, the 1023-amino acid polypeptide chain folds into five compact sequential domains, plus an extended segment of about 50 residues at the N-terminus. Each of the four active sites in the tetramer is formed by elements from two different subunits.[25] Recently, $\beta$GAL molecules have been investigated in our research group for label-free detection of single molecules and protein−protein interactions in the deep UV region after one-photon excitation at 266 nm.[8,10] AF350 dye is a sulfonated coumarin derivative with high fluorescence quantum yield (0.75).[26] The spectral absorption of AF350 overlaps with the fluorescence emission of the $\beta$GAL donor, which satisfies the basic requirement of resonance energy transfer. We have chosen AF350 as an acceptor also because of its advantage of exhibiting more intense fluorescence and higher photostability than many other dyes, remaining highly fluorescent over a broad pH range, and having good water solubility.[26,27] We report FRET studies after specific biotin−avidin binding events based on biotinylated $\beta$GAL and avidin-AF350. It is shown that basic information about the location of AF350 can be obtained. Further, the fluorescence energy transfer efficiency and average distance between donor and acceptor were determined by experiment and theoretical calculation. The fluorescence intensity image of AF350 on a biotinylated $\beta$GAL-coated quartz surface through UV FRET has been observed using deep UV laser-based fluorescence lifetime microscopy. We are able to demonstrate the sensitive identification of UV FRET from biotinylated $\beta$GAL to avidin-AF350 based on high binding affinity of a biotin−avidin reaction by deep UV laser-based fluorescence lifetime microscopy.

## 2. EXPERIMENTAL METHODS

**2.1. Materials.** The pure biotinylated $\beta$GAL, *N*-acetyl-L-tryptophanamide (NATA) and 3-aminopropyltriethoxysilane (APTES) were purchased from Sigma. AF350-conjugated avidin (NeutrAvidin) was purchased from Invitrogen (Molecular Probes). Biotinylated $\beta$GAL was solved and diluted in phosphate buffered saline solution (PBS, pH 7.4), and avidin-AF350 and NATA were solved and diluted in double distilled water. All other chemicals were of analytical grade.

**2.2. Sample preparation.** For absorption and steady-state fluorescence experiments, biotinylated $\beta$GAL concentration was kept constant at 2.25 $\mu$M, while avidin-AF350 concentration was varied to reach biotin $\beta$GAL:avidin-AF350 molar ratios of 1:0 to 1:3. Absorption spectra of solutions were measured with UV/visible/near-infrared (UV/vis/NIR)-spectroscopy (Lambda 900, Perkin-Elmer). Steady-state fluorescence spectra were obtained in standard quartz cuvettes with a luminescence spectrometer (LB 50B, Perkin-Elmer) equipped with a red-sensitive photomultiplier tube (Hamamatsu R-928). Time-resolved fluorescence spectroscopy of biotinylated $\beta$GAL and biotin−avidin complex solutions were measured with a homemade UV fluorescence lifetime microscope at a fluorescence detection window of 320−380 nm by putting a 100 $\mu$L sample on quartz cover slides that were glued to aluminum slabs with six reaction vessels containing a volumetric capacity of 300 $\mu$L. The experiments were performed at a constant biotinylated $\beta$GAL concentration of $1 \times 10^{-7}$ M, and the avidin-AF350 concentration was varied. Prior to use, the quartz cover slides (SPI Supplies, 170 $\mu$m thickness) were cleaned for 60 min in $CHCl_3$ in an ultrasonic bath followed by washing with double-distilled water and then dried in nitrogen flow. The fluorescence of NATA shows a single-exponential decay with lifetime of 2.85 ± 0.05 ns,[28] which was used as the standard to calibrate the instrument response. For the data analysis, commercial software FluoFit by PicoQuant was used. The experimental data were analyzed using the Marquardt−Levenberg algorithm. The decay parameters were determined by least-squares deconvolution using multiexponential models, and their quality was judged by the reduced $\chi^2$ value and the randomness of the weighted residuals. All experiments were performed at room temperature.

For UV FRET imaging experiments, quartz coverslips were cleaned in a 1:1 mixture of MeOH/HCl for 30 min and in concentrated $H_2SO_4$ for 30 min. They were rinsed with double-distilled water and dried in nitrogen flow. Afterward, the coverslips were deposited on 2.5% solution of APTES in ethanol for 30 min, rinsed with ethanol, and dried at 45 °C for 1 h. The APTES-coated coverslips were treated with biotinylated $\beta$GAL ($1 \times 10^{-6}$ M) in PBS solution overnight. After washing three times with water, they were placed in different concentration of avidin-AF350 solution for 1 h. Fluorescence imaging of AF350 on biotinylated $\beta$GAL quartz coverslips was measured using UV fluorescence lifetime imaging microscopy at a detection window of 430−470 nm after washing away any unbounded avidin-AF350 and drying coverslips in nitrogen flow.

**2.3. UV Fluorescence Lifetime Microscopy.** The time-resolved fluorescence studies were carried out with a UV fluorescence lifetime microscope described elsewhere.[8,9] It consists of a 266 nm UV mode-locked diode-pumped picosecond laser (GE-100-XHP-FHG, Time-Bandwidth Products Inc., Switzerland). The laser system provides pulses with a duration of less than 10 ps and with a repetition rate of 40 MHz, and the maximum output power is 20 mW. The polarized laser beam was split 50/50 by a beam splitter (Laser components GmbH, Germany) sending 50% into a high speed photodiode module (PHD-400, Becker & Hickl GmbH, Berlin, Germany), which is used as deriving the synchronization signal for triggering of the time-correlated single photon counting (TCSPC) module. The second beam passed an excitation filter (254WB25, Omega Optical) and is directed into the quartz microscope objective (40×, NA = 0.80, Partec GmbH, Münster, Germany) by a dichroic beamsplitter (290DCLP, Omega Optical). The laser power was adjusted by inserting different neutral density filters (Melles Griot). An automatic beam shutter is incorporated to minimize the unnecessary exposure time, which prevented the protein from bleaching. The fluorescence light was collected by the same objective and transmitted through the dichroic mirror. An achromatic lens (LAU-25-200, OFR Inc., 200 mm focal distance) focuses the light onto a pinhole. After the pinhole, the fluorescence emission is detected by a high speed photomultiplier tube (PMT) detector head (PMH-100-6, Becker & Hickl GmbH, Berlin, Germany). Emission bandpass filter 330WB60 (Omega Optical) have been used to detect Trp fluorescence and an emission bandpass filter FB450-40 (Thorlabs) used to discriminate acceptor fluorescence emission against donor fluorescence emission. The signal pulses of the PMT was fed into a TCSPC PC interface card (SPC-630, Becker & Hickl GmbH, Berlin, Germany) to acquire time-resolved data. The TCSPC was performed in the reversed mode, i.e., the signal of the PMT was used to start the clock of the time-to-amplitude converter, and the reference signal of the laser from a high speed photodiode was used as the stop signal. The instrument response function (IRF) was measured by replacing the sample with a scattering dispersion of colloidal silicon dioxide particles in water (particle size 11 nm), and then recording the Rayleigh scattering of the excitation light without two emission filters. With this setup, an IRF of 240 ps (fwhm) was measured. The fluorescence decay time constants were obtained by deconvoluting the IRF.

**2.4. Förster distance and energy transfer efficiency calculation.** The overlap integral $J(\lambda)$ expresses the degree of spectral overlap between the donor emission and the acceptor absorption,[1]

$$J(\lambda) = \int_0^\infty F_D(\lambda)\varepsilon_A(\lambda)\lambda^4 d\lambda = \frac{\int_0^\infty F_D(\lambda)\varepsilon_A(\lambda)\lambda^4 d\lambda}{\int_0^\infty F_D(\lambda)d\lambda} \quad (1)$$

$F_D(\lambda)$ is the corrected fluorescence intensity of the donor in the wavelength range $\lambda$ to $\lambda+\Delta\lambda$, with the total intensity normalized to unity; it is dimensionless. $\varepsilon_A(\lambda)$ is the extinction coefficient of the acceptor at $\lambda$, typically in units of $M^{-1}$ $cm^{-1}$. If $\lambda$ is expressed in units of centimeters, the $J(\lambda)$ is in units of $M^{-1}$ $cm^3$.

The Förster distance, $R_0$, can be calculate from the equation

$$R_0 = 9.78 \times 10^3(\kappa^2 n^{-4} Q_D J(\lambda))^{1/6} \quad (\text{in Å}) \quad (2)$$

where $\kappa^2$ is an orientation factor of two dipoles interacting and usually assumed to be equal to 2/3, $n$ is the refractive index of medium between donor and acceptor, $Q_D$ is the fluorescence quantum yield of donor in the absence of acceptor, and $J(\lambda)$ is the spectral overlap integral. The Förster distance $R_0$ is known as the distance at which the transfer rate is equal to the decay rate of the donor in the absence of acceptor. That is the separation distance that yields 50% energy transfer efficiency.[2]

The transfer efficiency ($E$) is typically measured using the relative fluorescence intensity of the donor, in the absence ($F_D$) and presence ($F_{DA}$) of acceptor:

$$E = 1 - \frac{F_{DA}}{F_D} \quad (3)$$

or the transfer efficiency ($E$) can also be calculated from the change of the fluorescence lifetime of the donor, in the absence ($\tau_D$) and presence ($\tau_{DA}$) of acceptor:

$$E = 1 - \frac{\tau_{DA}}{\tau_D} \quad (4)$$

The relation between the transfer efficiency ($E$), the Förster distance $R_0$, and the mean distance $r$ between the donor and acceptor is given by eq 5:

$$E = \frac{R_0^6}{R_0^6 + r^6} \quad (5)$$

## 3. RESULTS AND DISCUSSSION

The absorption and emission spectra of biotinylated $\beta$GAL and avidin-AF350 are shown in Figure 2a. Biotinylated $\beta$GAL acted as a multidonor system while avidin-AF350 was the acceptor fluorophore. Biotinylated $\beta$GAL was excited at 266 nm and has an emission peak at 341 nm, while avidin-AF350 has an excitation peak at 346 nm and an emission peak at ~440 nm. The emission band of the donor overlaps very well with the absorption of the acceptor, suggesting that efficient FRET between the biotinylated $\beta$GAL donor and avidin-AF350 acceptor can take place. By using the corrected emission spectrum of the donor with its area normalized to unity and the wavelength $\lambda$ in centimeter units, a spectral overlap integral $J(\lambda)$ of $1.87 \times 10^{-14}$ $M^{-1}$ $cm^3$ was calculated from eq 2. On the basis of the spectral overlap, the bulk quantum yield of the biotinylated $\beta$GAL, and the absorption coefficient of avidin-AF350, we estimate an average Förster distance $R_0$ of 29.3 Å in the biotinylated $\beta$GAL/avidin-AF350 FRET system.

Figure 2b shows the results of fluorescence energy transfer studies on biotinylated $\beta$GAL at pH 7.4 in the presence of different avidin-AF350 concentrations. Increasing the concentration of avidin-AF350 resulted in a decrease of the Trp fluorescence at 340 nm, concurrent with an increase in the fluorescence at 438 nm; the fluorescence signal of biotinylated $\beta$GAL shows almost no significant change when the avidin-AF350 to biotinylated $\beta$GAL ratio exceeds 3:1. Because free avidin-AF350 almost does not fluoresce when excited at 266 nm (Figure 2b dashed-line), the 438 nm band represents AF350 emission due to FRET when avidin-AF350 binds to biotinylated $\beta$GAL. Binding of avidin-AF350 to biotinylated $\beta$GAL resulted in a decrease of the intrinsic

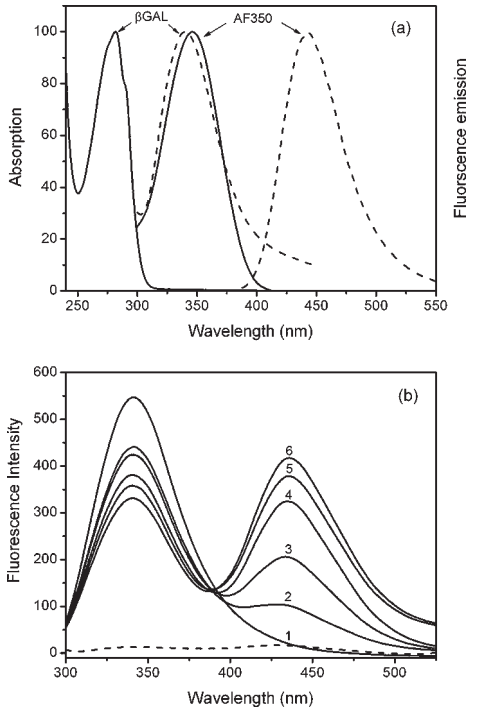


**Figure 2.** (a) Absorption (solid line) and fluorescence emission (dashed line) spectra of $\beta$GAL and AF350. The FRET spectral overlap integral $J(\lambda)$ is located between absorption spectrum of the acceptor and fluorescence emission spectrum of the donor. (b) Evolution of the corrected fluorescence emission intensity biotinylated $\beta$GAL and avidin-AF350 in the absence and presence of avidin-AF350 under excitation at 266 nm. The concentration of biotinylated $\beta$GAL is 2.25 $\mu$M, the molar ratios of biotinylated $\beta$GAL:avidin-AF350 (1→6) is 1:0, 1:0.4, 1:1., 1:1.5, 1:2, and 1:3, respectively. The dashed line shows the emission of avidin-AF350 acceptor without donor.

Trp fluorescence emission of approximate 39%. The experimental energy transfer efficiency calculated according to eq 3 is 39.4%. The experimental average distance $r$ between the donor and acceptor of 31.5 Å can be determined from eq 5 based on the value of $E$ and $R_0$.

The tetrametic $\beta$GAL is a relatively large protein with a diameter of roughly 100 Å,[25,29] and contains 156 Trp residues. Since $\beta$GAL fluorescence is largely overlapping with the AF350 absorbance spectrum, the mechanism of the energy transfer from Trp to the AF350 group must be the Förster type dipole−dipole interaction with $r^{-6}$ distance dependence. The theoretical efficiency of energy transfer is given by[30]

$$\langle E_{\text{ent}} \rangle = \frac{1}{n} \sum_{i=1}^{n} \left( \frac{R_0^6}{R_0^6 + r_i^6} \right) \qquad (6)$$

where $n$ is the total number of Trp groups in $\beta$GAL and avidin, $R_0$ is the Förster distance obtained from the spectral overlap between the fluorescence spectrum of $\beta$GAL and the absorption spectrum of AF350, and $r_i$ is the center-to-center distance from the $i$th Trp unit to the AF350 unit. The avidin molecule has four biotin-binding sites, which have almost the same binding behavior, i.e., they are considered to be random by chosen for binding.[16−18] We assume that the average position of AF350 is located in the center of the avidin molecule, because the potential labeling sites of AF350 (Lys, Arg, and Cys) are distributed over

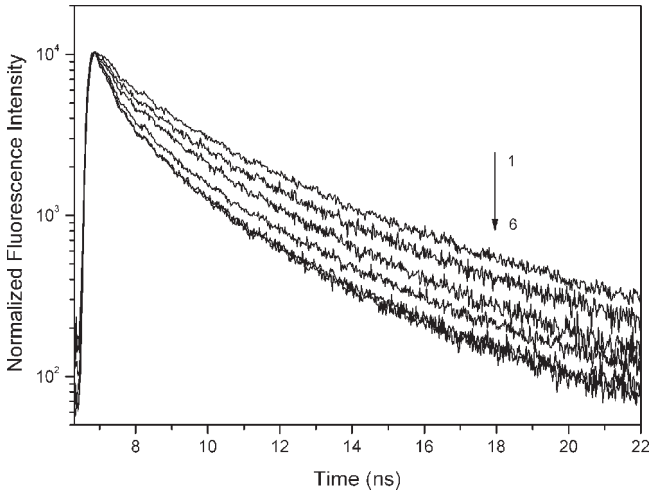


**Figure 3.** Time-resolved fluorescence decay of biotinylated $\beta$GAL in the absence and presence of avidin-AF350 in PBS buffer solution (pH 7.4) under excitation at 266 nm. Biotinylated $\beta$GAL concentration was fixed at 0.1 $\mu$M, and the molar ratios of biotinylated $\beta$GAL:avidin-AF350 (1→6) are 1:0, 1:0.4, 1:1., 1:1.5, 1:2, and 1:3, respectively.

the avidin molecule[31−33] more or less equally, and the four identical biotin-binding sites are symmetrically distributed on the avidin surface. The locations of Trp units were obtained from X-ray crystallographic data[25,34] and used to calculate the distance of $r_i$. The theoretical energy transfer efficiency calculated from eq 6 is 20.3%, which corresponds to a theoretical average distance between donor and acceptor to be 36.8 Å if we suggest a direct surface-to-surface contact of both proteins, i.e., the protein−protein distance is zero after binding. Compared to the experimental average distance of 31.5 Å, the calculated average distance between donor and acceptor is 5.3 Å longer, which is about four carbon−carbon bond lengths only. The basis for the calculation was a sphere−sphere contact assumption without any change of the sphere geometry due to binding. This slight difference might result from a conformational change in the protein after the binding event;[35] in other words, the protein−protein distance after binding is less than zero due to the close interaction.

Upon excitation at 266 nm, biotinylated $\beta$GAL displays an intrinsic fluorescence emission band around 340 nm mainly due to Trp residues. The fluorescence decay characterization of biotinylated $\beta$GAL in the absence and presence of avidin-AF350 in PBS buffer solution at pH 7.4 is shown in Figure 3. With gradual addition of acceptor avidin-AF350, the fluorescence decays of biotinylated $\beta$GAL donor become fast. The fluorescence decay curves can be fitted well with a triple-exponential decay function. The lifetime, relative amplitudes and the reduced $\chi^2$ value of the decay of biotinylated $\beta$GAL/avidin-AF350 system obtained by global analysis with three-exponential fit are listed in Table 1. Figure 4a shows the fitting curve for the fluorescence decay of biotinylated $\beta$GAL donor together with the IRF of our instrument. Analysis of the fluorescence decay data showed three components with significant different decay times of 5.11, 2.53, and 0.91 ns, the average fluorescence lifetime of biotinylated $\beta$GAL is 3.68 ns. The lower panel in Figure 4a shows weighted residuals of the triple-exponential fitting. The increase of avidin-AF350 concentration decreases the fluorescence lifetime of the donor, and the fluorescence decay of the donor remains unchanged when the molar ratio of biotinylated $\beta$GAL:avidin-AF350

**Table 1. The Intrinsic Fluorescence Intensity Decay Parameters of Biotinylated βGAL in the Absence and Presence of Avidin-AF350 in PBS Buffer Solution (pH 7.4)**

| biotinylated βGAL:avidin-AF350 | <τ> | $\alpha_1$ | $\tau_1$ | $\alpha_2$ | $\tau_2$ | $\alpha_3$ | $\tau_3$ | $\chi^2$ |
|---|---|---|---|---|---|---|---|---|
| 1:0 | 3.68 | 0.27 | 5.11 | 0.28 | 2.53 | 0.45 | 0.91 | 2.1 |
| 1:0.4 | 3.36 | 0.24 | 4.84 | 0.36 | 1.93 | 0.40 | 0.66 | 1.4 |
| 1:1 | 2.92 | 0.22 | 4.25 | 0.40 | 1.56 | 0.38 | 0.46 | 1.8 |
| 1:1.5 | 2.64 | 0.16 | 4.16 | 0.30 | 1.49 | 0.55 | 0.40 | 1.7 |
| 1:2 | 2.43 | 0.13 | 3.92 | 0.29 | 1.35 | 0.58 | 0.35 | 2.0 |
| 1:3 | 2.33 | 0.12 | 3.88 | 0.29 | 1.31 | 0.58 | 0.34 | 1.9 |

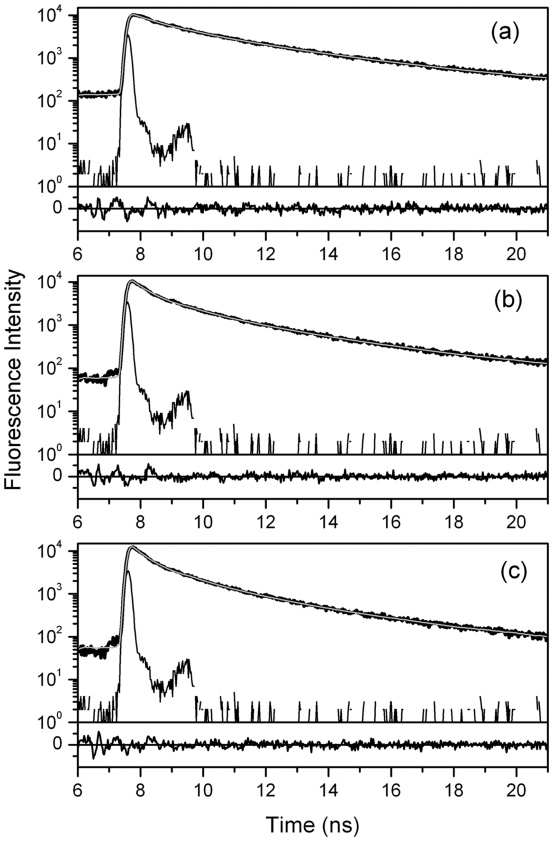


**Figure 4.** The triple-exponential decay fitting for the fluorescence decay of biotinylated βGAL in the presence of different molar ratios of avidin-AF350 in PBS buffer solution (pH 7.4) excited at 266 nm together with the IRF. The molar ratios of biotinylated βGAL:avidin-AF350 are (a) 1:0, (b) 1:1.5, (c) 1:3, respectively. The gray lines are fit curves to triple-exponential fluorescence decay. The lower panels show weighted residuals of each fitting.

reaches 1:3. The fluorescence lifetimes of the three components change to 3.88, 1.31, and 0.34 ns, and the average lifetime of donor decreases to 2.33 ns (Figure 4c). The average fluorescence lifetime of biotinylated βGAL decreases initially with the increasing acceptor-to-donor ratio in the conjugates, but quickly levels off at a ratio of 1:2, which is consistent with the changing levels of fluorescence intensity of donor. The FRET efficiency is improved according to the scheme model in which single avidin AF350 can be conjugated with multiple biotinylated βGAL. The energy transfer efficiency calculated from the average lifetime

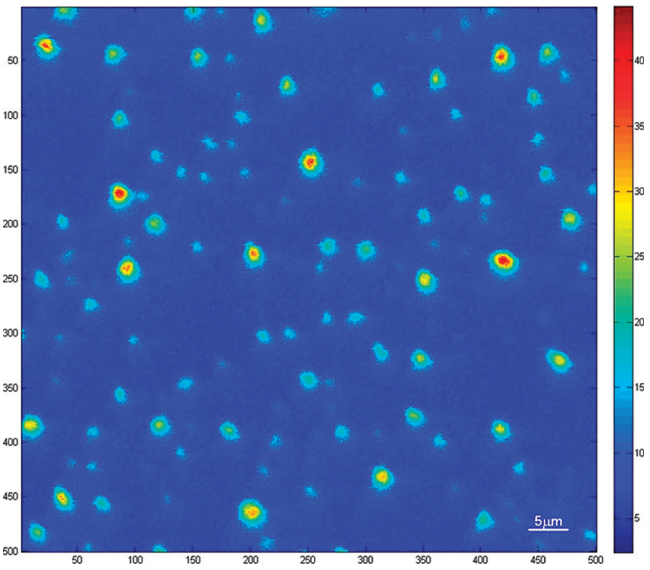


**Figure 5.** The fluorescence intensity image of AF350 on a biotinylated βGAL-coated quartz surface after UV FRET based on a biotin−avidin binding reaction. The biotinylated βGAL-coated quartz coveslips were placed in $1 \times 10^{-8}$ mol/L avidin-AF350 solution for 1 h. After washing away any unbounded avidin-AF350, the coverslips were measured by fluorescence imaging using UV fluorescence lifetime imaging microscopy at a detection window of 430−470 nm.

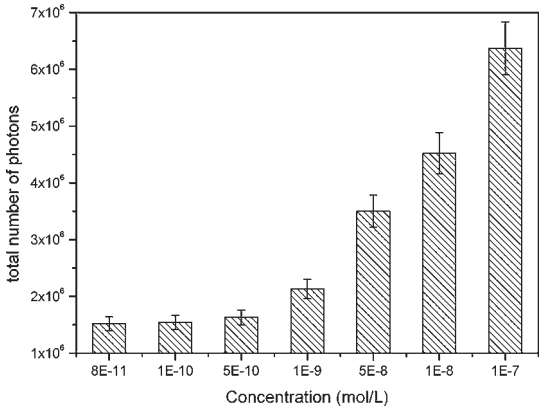


**Figure 6.** The dependence of the total number of photons counted from each fluorescence intensity image on different concentrations of the avidin-AF350 solution.

changes using eq 4 is to be 36.7%, which corresponds to the value obtained from the change of the donor emission intensity.

With the molecular system described here, deep UV FRET can be generated with small sample volumes and at low concentrations, respectively. Hence, label-free optical biosensors are possible based on FRET measurements between biotinylated βGAL and avidin-AF350 on surfaces. The fluorescence spots on a quartz surface have been observed at 266 nm excitation after adding avidin-AF350 to a biotinylated βGAL-coated quartz surface (Figure 5). The fluorescence image from AF350 emission indicates FRET between βGAL and AF350 after the biotin−avidin binding reaction. The enery transfer efficiency depends not only on the distance between donor and acceptor fluorphores, but also on their relative orientation in space of the transition dipoles. Although the orientation of biotinylated

βGAL on the surface is unknown, it might not have significant influence on the energy transfer efficiency between βGAL and AF350, because many Trp residues in βGAL protein served as donors, and they have different orientations. The orientation of the transition dipoles between the multidonor and acceptor can take a dynamically random average, i.e., orientation factor $\kappa^2$ is equal to 2/3. In order to quantify the sensitivity of our method for UV FRET based on biotin−avidin binding reaction, different concentrations of the avidin-AF350 solution were placed on biotinylated βGAL-coated quartz coverslips, and we measured the dependence of the total number of photons counted from each fluorescence intensity image on different concentrations of the avidin-AF350 solution (Figure 6). We did not observe any fluorescence spots on quartz surfaces at avidin-AF350 concentrations less than $5 \times 10^{-10}$ mol/L; the recorded fluorescence represents the background level. We observed fluorescence spots above the background level on quartz surfaces at avidin-AF350 concentrations higher than $1 \times 10^{-9}$ mol/L, which indicates that we are able to study intermolecular interactions at low concentrations (down to nanomolar range) with this method.

## 4. CONCLUSIONS

Deep UV FRET measurements between βGAL and AF350 based on biotin−avidin binding reactions have been demonstrated in our experiment by means of steady-state fluorescence and time-resolved fluorescence spectroscopy. Our method uses the intrinsic Trp residues in biotinylated βGAL proteins to serve as the FRET donor. The fluorescence decay of biotinylated βGAL in the presence of different concentrations of avidin-AF350 was analyzed by reconstructing the decay time distributions with multiexponential models. The effect of FRET leads to a decrease of the mean fluorescence lifetime from 3.68 to 2.33 ns. The fluorescence energy transfer efficiency was determined by the donor fluorescence emission and lifetime changes in the presence and absence of acceptor. The theoretical efficiency of energy transfer and the theoretical average distance between donor and acceptor are calculated, and the results show good agreement with the experimental data even without knowing the accurate orientation of the donors in the molecule. In other words, this method allows obtaining some structural data (the average distance between ligand and receptor after binding) in even such a complex system; neither specific information about the ligand and receptor nor site-specific labeling is necessary. Smaller molecular systems will allow obtaining even more information (e.g., rotational freedom). This we have to show in future work.

The fluorescence intensity image of AF350 on a biotinylated βGAL-coated quartz surface through UV FRET has been observed using deep UV laser-based fluorescence lifetime microscopy. The results demonstrate that deep UV laser-based fluorescence lifetime microscopy is useful for the study of UV fluorescence energy transfer from biotinylated βGAL to avidin-AF350 based on the high binding affinity of biotin−avidin reaction. With this molecular system we have shown that ultrasensitive confocal time-resolved deep UV fluorescence microscopy is a useful tool to study intermolecular interactions at very low concentrations in solution and on a surface. Since deep UV light excitation is phototoxic to biological samples, multiphoton excitation label-free fluorescence detection can be used for living samples or in cases where the samples have to be preserved for further investigations. Excitation light in multiphoton excitation has a longer wavelength, which is less phototoxic to living cells and can penetrate deeper into the specimen. Ultrasensitive optical biosensors with label-free detection can be developed for life sciences analysis without modifying molecules of interest and enables the use of natural ligands and substrates.

## AUTHOR INFORMATION

### Corresponding Author

*Tel: +41-44-6354451. Fax: +41- 44 −6356813. E-mail: sseeger@pci.uzh.ch.

## ACKNOWLEDGMENT

The authors thank the Swiss National Science Foundation for financial support and research grants.

## REFERENCES

(1) Lakowicz, J. R. *Principles of Fluorescence Spectroscopy*, 3rd ed.; Springer: New York, 2006.
(2) Förster, T. In *Modern Quantum Chemistry*; Sinanoglu, O., Ed.; Academic Press: New York, 1965; pp 93−137.
(3) Stryer, L. *Annu. Rev. Biochem.* **1978**, *47*, 819–846.
(4) Wu, P. G.; Brand, L. *Anal. Biochem.* **1994**, *218*, 1–13.
(5) dos Remedios, C. G.; Moens, P. D. J. In *Resonance Energy Transfer*; Andrews, D. L., Demidov, A. A., Eds.; John Wiley & Sons: Chichester, England, 1999; pp 1−64.
(6) Gorbenko, G. P.; Domanov, Y. A. *J. Biochem. Biophys. Methods* **2002**, *52*, 45–58.
(7) Li, Q.; Seeger, S. *Appl. Spectrosc. Rev.* **2010**, *45*, 12–43.
(8) Li, Q.; Seeger, S. *Anal. Chem.* **2006**, *78*, 2732–2737.
(9) Li, Q.; Ruckstuhl, T.; Seeger, S. *J. Phys. Chem. B* **2004**, *108*, 8324–8329.
(10) Li, Q.; Seeger, S. *Anal. Biochem.* **2007**, *367*, 104–110.
(11) Li, Q.; Seeger, S. *Sens. Actuators, B* **2009**, *139*, 118–124.
(12) Riaplov, E.; Li, Q.; Seeger, S. *Protein Pept. Lett.* **2007**, *14*, 712–715.
(13) Belin, G. K.; Seeger, S. *Electrophoresis* **2009**, *30*, 2565–2571.
(14) Belin, G. K.; Seeger, S. *J. Nanosci. Nanotechnol.* **2009**, *9*, 2645–2650.
(15) Zauner, G.; Lonardi, E.; Bubacco, L.; Aartsma, T. J.; Canters, G. W.; Tepper, A. *Chem.—Eur. J.* **2007**, *13*, 7085–7090.
(16) Green, N. M. *Biochem. J.* **1964**, *90*, 564–568.
(17) Green, N. M. *Biochem. J.* **1966**, *101*, 774–780.
(18) Green, N. M. In *Adv. Protein Chem.*; Anfinsen, C. B., Edsall, J. T., Richards, F. M., Eds.; Academic Press: New York, 1975; Vol. 29; pp 85−133.
(19) Wilchek, M.; Bayer, E. A. *Biomol. Eng.* **1999**, *16*, 1–4.
(20) Qin, Q. P.; Lovgren, T.; Pettersson, K. *Anal. Chem.* **2001**, *73*, 1521–1529.
(21) Savage, M. D.; Mattson, G.; Desai, S.; Nielander, G.; Morgensen, S.; Conklin, E. J. *Avidin−Biotin Chemistry: A Handbook*; Pierce: Rockford IL, 1992.
(22) Wilchek, M.; Bayer, E. A. In *Avidin−Biotin Technology, Methods in Enzymology*; Academic Press: San Diego, 1990; Vol. 184; pp 746.
(23) Klein, G.; Humbert, N.; Gradinaru, J.; Ivanova, A.; Gilardoni, F.; Rusbandi, U. E.; Ward, T. R. *Angew. Chem., Int. Ed.* **2005**, *44*, 7764–7767.
(24) Chew, Y. C.; Sarath, G.; Zempleni, J. *J. Nutr. Biochem.* **2007**, *18*, 475–481.
(25) Jacobson, R. H.; Zhang, X. J.; Dubose, R. F.; Matthews, B. W. *Nature* **1994**, *369*, 761–766.
(26) Panchuk-Voloshina, N.; Haugland, R. P.; Bishop-Stewart, J.; Bhalgat, M. K.; Millard, P. J.; Mao, F.; Leung, W. Y.; Haugland, R. P. *J. Histochem. Cytochem.* **1999**, *47*, 1179–1188.
(27) Haugland, R. P. *Handbook of Fluorescence Probes and Research Products*, 9th ed.; Molecular Probes, Inc.: Eugene, OR, 2002.
(28) Andrade, S. M.; Carvalho, T. I.; Viseu, M. I.; Costa, S. M. B. *Eur. J. Biochem.* **2004**, *271*, 734–744.

(29) Karlsson, U.; Sjostrand, F. S.; Koorajia, S; Miller, A.; Zabin, I. *J. Ultra. Res.* **1964**, *10*, 457–469.
(30) Kuragaki, M.; Sisido, M. *Bull. Chem. Soc. Jpn.* **1997**, *70*, 261–265.
(31) Livnah, O.; Bayer, E. A.; Wilchek, M.; Sussman, J. L. *Proc. Natl. Acad. Sci. U.S.A.* **1993**, *90*, 5076–5080.
(32) Pugliese, L.; Coda, A.; Malcovati, M.; Bolognesi, M. *J. Mol. Biol.* **1993**, *231*, 698–710.
(33) Rosano, C.; Arosio, P.; Bolognesi, M. *Biomol. Eng.* **1999**, *16*, 5–12.
(34) Matthews, B. W. *C. R. Biol.* **2005**, *328*, 549–556.
(35) Koshland, D. E. *Proc. Natl. Acad. Sci. U.S.A.* **1958**, *44*, 98–104.